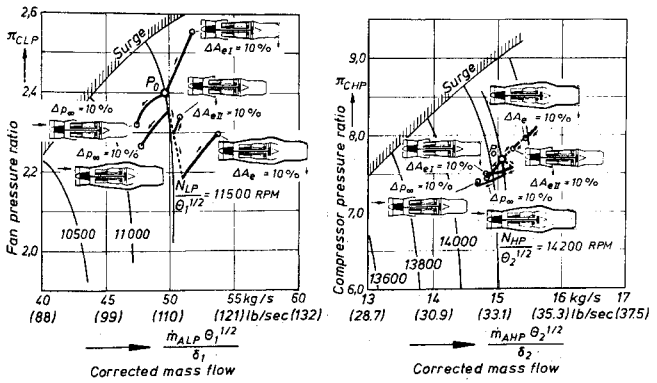

Fig. 9 Fan and compressor operation with step increases in low-pressure air bleed $\dot{m}_{BLP}$ and high pressure air bleed $\dot{m}_{BHP}$.

according to Eq. (8), as variables, the accuracy of calculation is improved. Eq. (9) enables the determination of any variable of additional interest, which may be formulated from the variables already introduced in the system from Eqs. (2–8).

Of particular importance are the instationary elements of the system of equations, which influence the transient characteristics of the dependent variables, but not their final steady-state value. The effect of these shares is dependent upon the storage capacity of the components and structures concerned and on the time required to fill and drain the capacity.

For the determination of all nonstationary processes caused by brief interferences in the order of a few seconds, it is sufficient to take into account merely the energy accumulating rotor to obtain a satisfactory approximation.

References

[1] Pearson, H., "Mixing of Exhaust and Bypass Flow in a Bypass Engine," *Journal of the Royal Aeronautical Society*, Vol. 66, Aug. 1962, pp. 528–530.

[2] Heiser, W. H., "Thrust Augmentation," *Transactions ASME, Ser. A*, Vol. 89, 1967, pp. 75–82.

[3] Dettmering, W. and Fett, F., "Methoden der Schuberhöhung und ihre Bewertung," *Zeitschrift für Flugwissenschaften*, Vol. 17, No. 8, Aug. 1969, pp. 257–267.

[4] Fett, F., "The Dynamic Behavior of Jet Engines under External and Internal Action," *Advanced Components for Turbojet Engines, Part 2*," Paper 31, AGARD Conference Proceedings 34, Sept. 1968.

[5] Bauerfeind, K., "Die Berechnung des Übertragungsverhaltens von Turbo-Strahltriebwerken unter Berücksichtigung des instationären Verhaltens der Komponenten," *Luftfahrttechnik-Raumfahrttechnik*, Vol. 14, No. 5 and No. 6, May and June 1968, pp. 117–124 and pp. 143–151.

[6] Greathouse, W. K., "Blending Propulsion with Airframe," *Space/Aeronautics*, Vol. 50, No. 6, Nov. 1968, pp. 59–68.

[7] Fett, F., "Das Regelverhalten von Strahltriebwerken," *Forschungsberichte des Landes Nordrhein-Westfalen*, No. 2065, Westdeutscher Verlag, Köln und Opladen, 1970.

OCTOBER 1971 J. AIRCRAFT VOL. 8, NO. 10

Exhaust Nozzle Drag: Engine vs Airplane Force Model

DAVE BERGMAN*
Convair Aerospace Division, General Dynamics Corporation, Fort Worth, Texas

A nozzle model which utilizes interchangeable internal and external parts was tested at high subsonic Mach numbers. Differences in nozzle drag brought about by the use of force- or reference-model exhaust conditions in contrast to engine conditions were investigated. In addition to typical designs, a number of alternative force-model nozzle (the type used in flow-through nacelles) variations were tested and evaluated. In general, force-model nozzle drag was found to be far different from that of the engine nozzles; however, some force-model variations did simulate the effects of engine flow at discrete operating conditions.

Nomenclature

A = cross-sectional area
C_D = boattail pressure drag coefficient (Drag/q_0A_m)
C_P = boattail pressure coefficient, $(P - P_0)/q_0$
D,d = diameter
h = boundary-layer height
L = length of boattail
M_0 = freestream Mach number
NPR = nozzle pressure ratio (P_{TJ}/P_0)
P,P_0 = local and freestream static pressure
P_{TJ} = exhaust jet total pressure
q = dynamic pressure
R = radius

Subscripts

B,b = boattail terminal plane
J = jet
M,m = maximum
0 = freestream
T = total

Introduction

AIRPLANE performance measurements, particularly those made during design and development stages, are acquired by applying a combination of experimental and analytical techniques rather than by using one specific device. This approach must be taken because, when considering an entire airplane configuration, each of these techniques has severe limitations, and the sole use of either will compromise accuracy in predicting airplane performance. As a result, an approach which systematically integrates both analytical and test results is normally used.

Presented as Paper 70-668 at the AIAA 6th Propulsion Joint Specialist Conference, San Diego, Calif., June 15–19, 1970; submitted June 29, 1970; revision received September 30, 1970.

* Propulsion Engineer, Aerospace Technology Department.

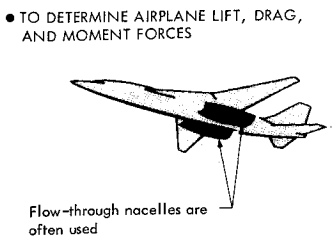

Fig. 1 Airplane force model.

The method for formulating a performance procedure generally is that of testing a scale airplane model which simulates as closely as possible the "real" airplane, and proceeding with analytical and semiempirical techniques to correct the test data in areas where true airplane simulation is lacking. The accuracy of such a procedure is dependent upon knowing what simulation errors do occur on test models and, moreover, why and to what degree errors are caused. Then the true applicability of model test data is made clear, and, additionally, data corrections can be accurately referenced to the respective simulation errors contained in the data.

Problem Statement

Measurements involving airplane aerodynamic forces (lift, drag, and moments) are made on what is commonly called an airplane "force" or "reference" model. As illustrated in Fig. 1, these scale models often have freestream "flow-through" nacelles that take the place of engine installations. An alternative approach is that of using "powered" nacelles (e.g., nacelles containing miniature gas turbines or gas ejectors); however, factors such as the relative complexity, high cost, and physical size of powered nacelles can sometimes bar their use. Most important, the use of flow-through nacelles means an incorrect, limited simulation of airplane internal/external flow interactions which occur during actual engine operation. The nacelle inlet and exhaust nozzle significantly influence surrounding flow and, thereby, affect nearby airframe forces. To help correct for this inexact simulation, other models (having high-pressure exhausts and capped inlets) designed to provide airframe performance *increments* may be used in addition to the necessary analytical corrections, such as scale effects.

Specifically, the subject to be discussed here concerns the engine exhaust nozzle and the related effects of its simulation. The sketch in Fig. 2 depicts the differences in nozzle geometry between an engine plug-type nozzle representative of subsonic cruise and its force-model nozzle counterpart. In the subsonic cruise position, the nozzle exterior surface (or "boattail") has a large amount of aft-facing projected area, thus causing a potential high-drag problem. Notice in Fig. 2 that while the external shape can be kept common to both nozzles, the centerbody plugs are quite different. Whereas the engine plug is designed to create a sonic throat at the exit plane and then allow flow expansion along the plug, the force-model nozzle has a smaller, truncated plug used solely to control inlet mass flow of the flow-through nacelle. Another significant difference between the two nozzles is the low nozzle pressure ratio (exhaust jet total pressure to freestream static pressure) of the force-model nozzle. These mismatches in nozzle internal geometry and pressure ratio create a force-model exhaust flowfield unlike that of engine exhausts. Incorrect simulation of jet plume shape and entrainment means that pressure distributions on the force-model nozzle exterior and other nearby airplane structure are dissimilar from those experienced with high-pressure engine exhaust flow. One should note that no matter how closely internal and external force-model nozzle geometry is made to resemble the engine nozzle, there will still remain a mismatch in nozzle pressure ratio which will result in the engine exhaust flowfield not being simulated.[1]

It follows that there is a need not only to know the simulation errors that occur with typical force-model nozzles but also to investigate any force-model nozzle "variations" which, perhaps, can cause the airplane flowfield to resemble that associated with the presence of engine exhaust flow. The goal of such an investigation is to reduce force-model simulation errors. Force-model nozzle variations such as centerbody contours, centerbody extensions, and the addition of cylindrical tube extensions are the candidates considered.

Method of Approach

External drag evaluation of a typical force-model nozzle and of variations on its design was done on an isolated basis in order to obtain generalized results. The results can be used as a reference to precede analyses with specific airframes in mind. Because of the limited objectives involved in an isolated-nozzle approach and also because of the complex internal/external flow interactions which occur, it was decided to obtain results mainly through use of experimental techniques.

A configuration representative of an engine plug-type nozzle for airplane subsonic cruise was used as the baseline nozzle. Wind-tunnel tests were conducted in the following manner: 1) The engine nozzle was tested at engine pressure ratios and, afterwards, 2) the same nozzle external shape was tested but with internal geometry and pressure ratios associated with flow-through nacelles, 3) the boattail pressure drag for each of the above conditions was measured, and the difference between the two drag levels indicated the amount of simulation error brought about by the force-model exhaust conditions.

Several force-model nozzle sleeve extensions and centerbody plug variations were tried with the desire that they might produce external flowfields similar to those with jet engine exhausts; however, the practical consideration was maintained that such variations should not add more external projected area than exists on the unmodified force-model nozzle. Thus, at zero angle of attack, the drag forces on the variations themselves would be only due to friction, which could be analytically determined and then easily accounted for in airplane test data.

Flow-through nacelles can be made to flow at various inlet capture-area ratios by varying the amount of internal nacelle blockage (e.g., changing the diameter of the nozzle plug). To observe this effect on the exhaust nozzle, more than one force-model nozzle plug diameter was tested. In addition, plug contours were varied so that any resultant changes in external drag could be examined. Several axial extensions of the

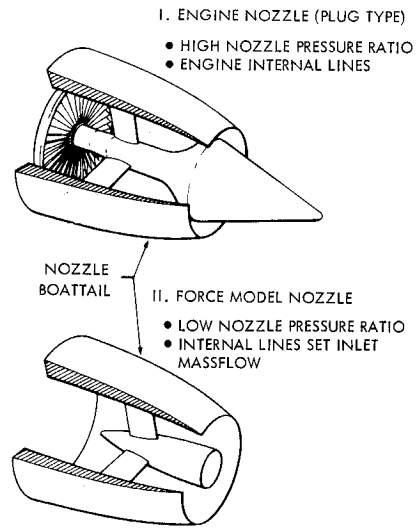

Fig. 2 A comparison of engine nozzle and force-model nozzle geometry.

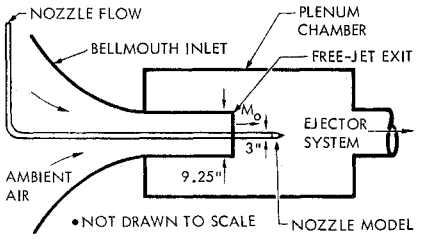

Fig. 3 Schematic of freejet wind tunnel.

force-model nozzle plug were tested. Also, the effect of adding hollow sleeve extensions to the nozzle was investigated as a means to adjust the external flowfield.

Model Test Technique

The nozzles were tested at several subsonic freestream Mach numbers and through a range of nozzle pressure ratios. Boattail drag measurements were made by instrumenting the model with static pressure orifices. Data from the orifices were used to determine boattail pressure distribution and, when integrated over the projected area, to provide boattail pressure drag.

Specifically, tests were conducted at Mach numbers of 0.55, 0.70, and 0.85, while nozzle exhaust flow ranged from jet-off to a pressure ratio of 4. The models were non ejector types; thus, there were no secondary flows. All configurations retained the minimum internal flow area at the nozzle exit plane.

Description of Test Facilities

Tests were conducted in a freejet wind-tunnel facility at the Convair Aerospace Division. A schematic of the tunnel is presented in Fig. 3. Ambient air, which is first drawn into a bellmouth inlet, flows through a smaller, square-shaped channel that connects to a large plenum chamber. It is at this point that a freejet test section is formed. Located here, the model becomes surrounded by high-velocity "freestream" flow. Various tunnel pressure data are measured by a scanivalve system and then reduced into final form by an on-line computer system.

A hollow pipe of circular cross section is used both to support the model and to deliver pressurized nozzle flow. Total pressure surveys of the pipe show a turbulent boundary layer with a height equal to approximately 17% of the model diameter ($h/d_m \approx 0.17$) at the nozzle connect point. This approximates the boundary-layer thickness for a fuselage installation, while a pod-type nozzle mounting would normally involve less boundary-layer growth.

Model and Instrumentation

The model geometry is shown in Fig. 4. A unique design feature of the model is the interchangeable geometry provision for accommodating several centerbody plugs and cylindrical sleeve extensions. In this manner, changes to the nozzle could be made while retaining the identical external boattail. Centerbody plugs attach to an internal support strut by means of a threaded connection, while the sleeve extensions could be slid into place and then locked by set-screws.

The 3-in.-diam nozzle has a circular-arc boattail shape with an 8° chordal angle (angle formed between centerline and line connecting the boattail start with the boattail trailing edge) and a 16° trailing-edge local angle. The engine centerbody plug has a 15° half-angle conical shape. Note that typical force-model nozzle centerbody plugs are truncated at the nozzle exit plane, so that plug drag can be easily measured apart from over-all airplane drag by either relatively few pressure orifices in the plug base or by a pressure probe device. The external boattail surface contains 30 static pressure orifices distributed along four rows separated by 90° quadrants. Model internal instrumentation includes three strut-mounted total-pressure tubes for determining nozzle pressure ratio (Fig. 5).

Results

The boattail configuration with the long cylindrical extension is similar to a model tested by NASA/Lewis.[2] Figure 6 shows excellent agreement, both in level and trend, between our data and NASA data for boattail pressures.

Plots of boattail pressure coefficient C_p vs the ratio of local to maximum cross-sectional area A/A_m are presented in Fig. 7. With this type of plot, the integral beneath the curve defines the boattail drag coefficient. Although each of the pressure distributions has typical boattail flow expansion-recompression trends, it is evident that changes in exhaust conditions have a considerable effect on boattail pressure levels. For example, the nozzle with the engine conical plug imparts only partial flow recompression on the boattail as opposed to the nozzle with the long, axial plug.

Boattail drag coefficients as functions of nozzle pressure ratio are summarized in Figs. 8 and 9. Notice that at exhaust flow velocities approximating the freestream velocity (NPR ≈ 1.6 for $M_0 = 0.85$) the long, axial plug (Centerbody 4) cre-

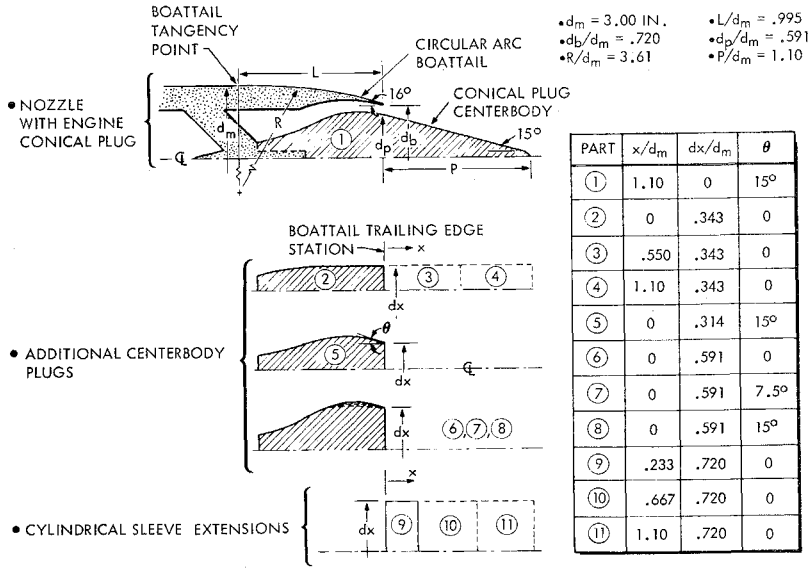

PART	x/d_m	dx/d_m	θ
①	1.10	0	15°
②	0	.343	0
③	.550	.343	0
④	1.10	.343	0
⑤	0	.314	15°
⑥	0	.591	0
⑦	0	.591	7.5°
⑧	0	.591	15°
⑨	.233	.720	0
⑩	.667	.720	0
⑪	1.10	.720	0

Fig. 4 Model parts description.

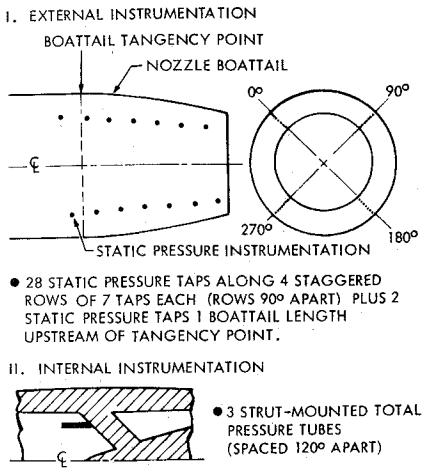

Fig. 5 Model instrumentation.

ated the same external drag effect as that of the long, cylindrical extension (Extension 11). As a result, it is felt that Centerbody 4 is of sufficient length to produce axial exhaust flow similar to a convergent, nonplug nozzle. Subsequently, comparisons were made which utilized Centerbody 4 to represent boattail drag levels with "convergent nozzle" flow. It is emphasized that these comparisons were made merely to highlight the strong effects on boattail drag caused by changes in jet plume shape. In contrast, an effort to determine the overall performance merits of one engine nozzle type vs another would involve accounting for internal thrust coefficients, centerbody plug forces, and the fact that plug vs nonplug nozzles of the same thrust class (equal jet areas) require different amounts of boattail projected area.

As seen in Fig. 8, the engine conical plug causes considerably more boattail drag than does the convergent nozzle (both nozzles having the same boattail geometry). Because conical plug nozzle exhaust flow is aimed down along the centerbody, the jet plume shape is quite different compared to the axially-directed exhaust flow. Therefore, flow on the boattail is recompressed to a greater extent in the presence of the convergent nozzle jet exhaust. For the plug nozzle, further recompression of the external flow normally occurs downstream of the boattail surface, adjacent to the centerbody plug. The engine plug force then benefits from the "aerodynamic boattail" recompression which takes place.

The dip in the drag coefficient vs NPR profile at nozzle subsonic exhaust flows ($1 < NPR < 1.89$) is due to the interaction of jet plume shape and jet entrainment effects. The presence of the plume causes boattail drag to be lowered significantly after initiation of exhaust flow but, as the jet velocity exceeds the surrounding flow velocity, an entrainment effect is also created which tends to speed up boattail flow, thereby lowering boattail pressures and increasing boattail drag. After the

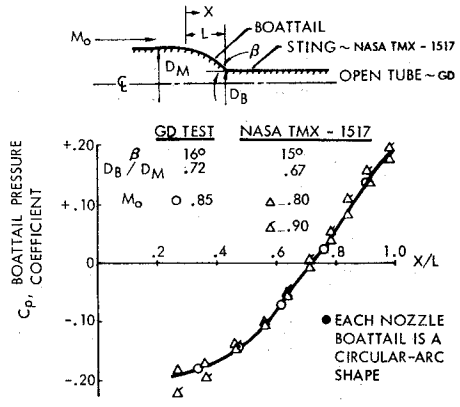

Fig. 6 Data substantiation.

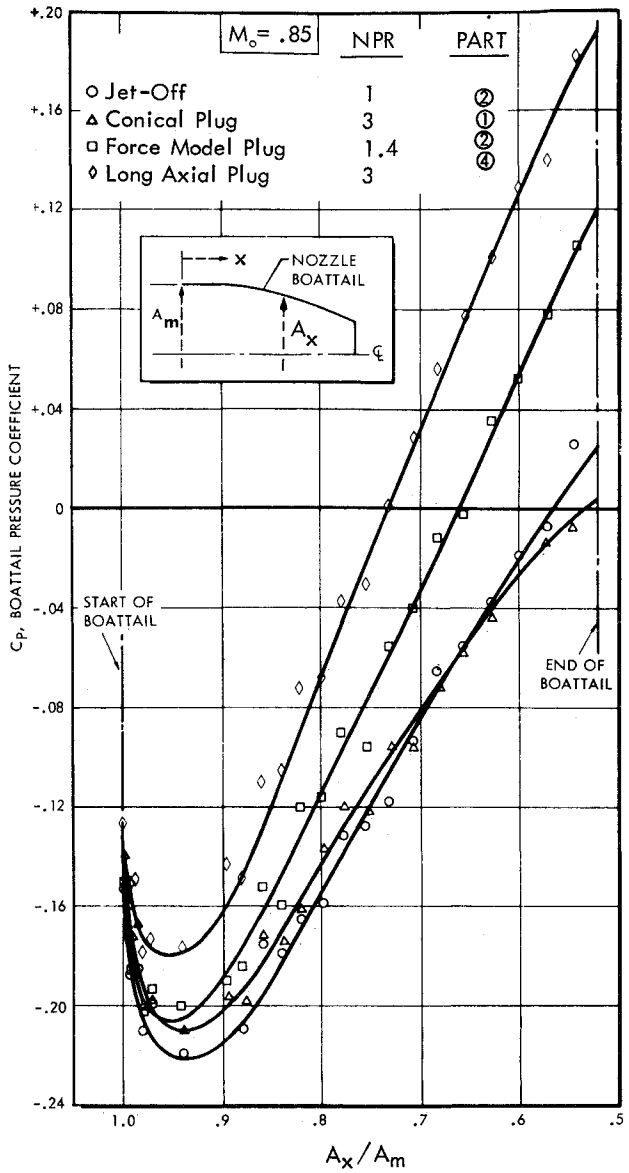

Fig. 7 Boattail pressure distribution.

exhaust flow becomes sonic ($NPR > 1.89$), the jet plume "billows out" beyond the exhaust area and the wide plume shape counteracts jet entrainment, thereby further reducing boattail drag.[1]

Extending the force-model plug beyond the nozzle exit plane causes sizeable changes in boattail drag as is shown in Fig. 9. These changes are in the direction of lowering drag with increases in plug length.

Adding cylindrical extensions (Fig. 9) also causes lower boattail drag levels. Not shown in Fig. 4 but present in these

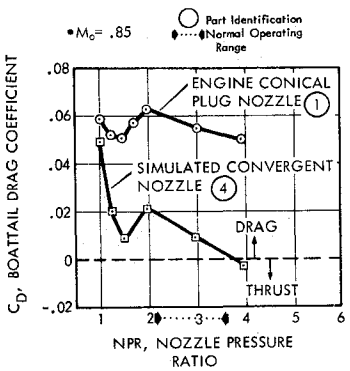

Fig. 8 Effect of high-pressure exhaust flow on boattail drag.

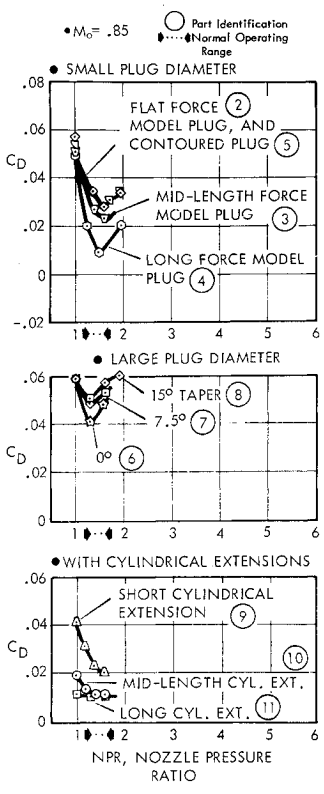

Fig. 9 Effect of force-model nozzle exhaust flow on boattail drag.

tests are axial force-model plugs inside each of the cylindrical extensions. These internal plugs are truncated at the cylinder exhaust plane and are sized to retain the identical exit flow area for all of the flow-through nacelle nozzles tested. Similar to the trend seen with centerbody extensions, the longer cylindrical extensions reduce drag more than do the shorter lengths.

Since the tests were conducted at several freestream Mach numbers, it was possible to record any differences in boattail drag coefficient caused by changes in Mach number. Drag coefficients vs freestream Mach number are shown in Fig. 10. For the range of Mach numbers 0.55–0.85, boattail drag coefficient remains essentially constant for the configuration with the long cylindrical extension. In contrast, with the extension removed and no jet flow present, boattail drag coefficient increases with Mach number. It is felt that the jet-off drag increase is due to the boattail being subjected to only part of the expansion-recompression boattail flowfield, with remaining recompression occurring downstream of the nozzle. Additionally, the higher the freestream Mach number, the more boattail flow expansion occurs and, unlike the configuration with the cylindrical extension attached where the boattail can recover recompression on its own surface, the boattail with the jet-off conditions undergoes an early increase in drag coefficient with Mach number.

The bar chart of Fig. 11 illustrates the significant difference between the drag level of the typical force-model nozzle and the drag levels of high pressure-ratio nozzles with identical external contours. Force-model drag coefficients are presented for both a 90% and 100% nacelle flow recovery (recovery $=P_{T_J}/P_{T_0}$). Less than 100% recovery is shown

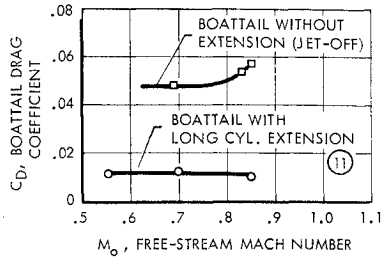

Fig. 10 Boattail drag vs Mach number.

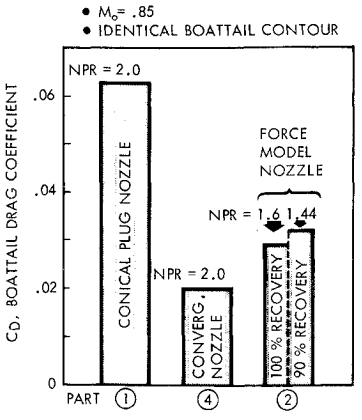

Fig. 11 Nozzle drag comparison.

since the exhaust from a flow-through nacelle will have a somewhat lower total pressure than that of the freestream because of nacelle duct losses.

Analysis

A description of the effects of varying the diameter of the force-model nozzle plug is given in Fig. 12. This description is important because several different centerbody plug diameters may be used during an airplane force-model test in order to vary inlet capture area. As seen in the figure, changes in plug diameter are strongly felt on the boattail. Boattail drag quickly approaches the high-drag, jet-off level as plug diameter is increased. This effect is apparently due to the abnormally narrow exhaust plume formed as the exhaust flow enters the area behind the blunt base. The external boattail flow is then abruptly directed toward the centerline aft of the nozzle exit. This effect causes high boattail drag by allowing a portion of the external flow recompression to occur downstream of the boattail. Nozzle pressure ratios of 1.4 and 1.6 are used in the figure to provide a recovery band for force-model-nozzle drag coefficients so as to account, in general, for flow-through-nacelle duct losses.

The effects of extending the length of the force-model nozzle plug are shown in Fig. 13. Note that boattail drag is significantly reduced as centerbody plugs are extended aft of the nozzle exit. These results indicate that locating the blunt base downstream from the boattail effectively causes a wide plume shape next to the boattail and a narrower plume shape at the base that, with added plug length, interferes less with the boattail. In regard to force-model nozzles simulating engine nozzle drag levels, the long plug (Centerbody 4) results in the same boattail drag as that of the convergent nozzle operating at a nozzle pressure ratio of approximately 3. From the results of the other plugs, one can predict that plug lengths somewhere between those of Centerbodies 3 and 4 could simulate the boattail drag of the convergent nozzle at pressure ratios between 2.0 and 3.0.

In order for the force-model nozzle to simulate the boattail drag of the engine conical-plug nozzle, the drag of the typical force-model nozzle must be increased (see Fig. 11). Recontouring the force-model centerbody plug was a possible means

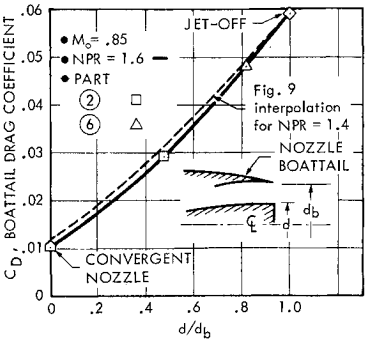

Fig. 12 Varying the plug diameter of the force-model nozzle.

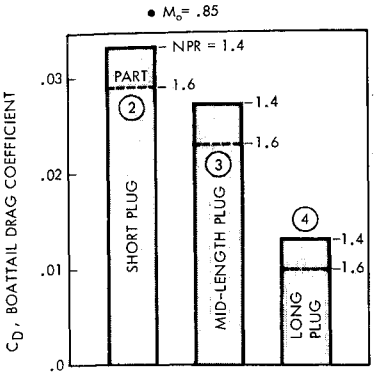

Fig. 13 Varying the force-model nozzle plug length.

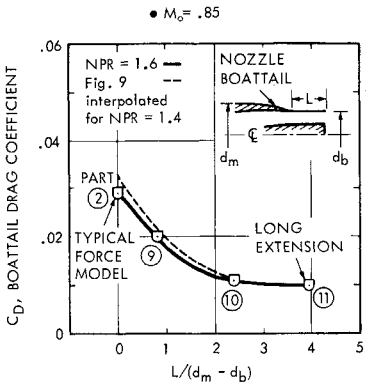

Fig. 15 Effects of cylindrical extensions on force-model nozzles.

and was tried on both the small- and large-diameter plugs. Presented in Fig. 14, the results show that boattail drag with the large-diameter plugs is sensitive to changes in plug contour, while drag with the small-diameter plugs is somewhat insensitive to contouring. For the large plugs, aiming the exhaust flow toward the centerline by recontouring the plug apparently creates a thinner plume shape near the boattail by allowing the exhaust to flow more directly into the base area region. However, typical force-model nozzles have centerbody plug diameters more in keeping with the small-diameter plugs tested; therefore, in practical use, force-model plug contouring seems to be a rather ineffective means for adjusting boattail drag.

The results of attaching cylindrical sleeves to the force-model nozzle, given in Fig. 15, show that boattail drag decreases with increasing cylindrical extension length. However, Extensions 10 and 11 each produce approximately the same drag levels. Thus, for the model tested, extensions any longer than Extension 11 would probably be no more effective in reducing drag. The short cylindrical sleeve (Extension 9) results in the same boattail drag as that of the convergent nozzle at NPR of 2, while the midlength and long cylinders (Extensions 10 and 11) simulate convergent nozzle drag at an NPR of 3. Note that the centerbody plug extensions and the cylindrical sleeve extensions each provide an effective means for adjusting force-model drag levels to those of the high-exhaust-pressure convergent nozzle. However, the sleeve extensions have the added feature of being adaptable to force models whether or not the force-model nozzles incorporate centerbody plugs.

Associated with the use of force-model nozzle extensions are some practical limitations. Use of nozzle extensions on airplane models must include many considerations, among which are restrictions in angle of attack, skin friction corrections, and the channeling effects of closely spaced extensions.

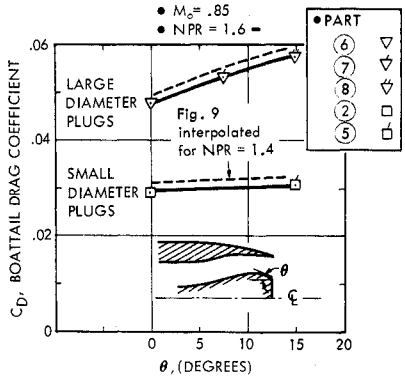

Fig. 14 Effect of force-model nozzle plug contour.

Conclusions

Subsonic wind-tunnel tests were conducted to determine the effects of nozzle drag brought about by the use of flow-through nacelles in airplane force models. The following conclusions are based on the configurations tested:

1) The boattail drag level of the nozzle with typical force-model exhaust flow is far different from that of the nozzle with either an engine plug-type or convergent-type exhaust.

2) All the nozzles tested have lower drag levels with the subsonic exhaust (low-nozzle-pressure ratios) than with the sonic exhaust and slightly higher pressure ratios. This phenomenon appears to be due to reduced jet entrainment effects when operating at low exhaust flow velocities.

3) The diameter of the force-model plug influences boattail flow. As the plug diameter is increased, boattail drag approaches the jet-off level. This illustrates that changes in flow-through-nacelle mass-flow setting can alter nozzle drag; this necessitates careful scrutiny, e.g., if the nozzle plug is changed when measuring inlet drag (varying capture-area ratio), then both inlet and nozzle drag changes will occur.

4) The technique of adding either centerbody plug or cylindrical sleeve extensions to the force-model nozzle produces favorable results in simulating the boattail drag of the high-pressure ratio convergent nozzle. Even though there are practical limitations to its use, this method may prove valuable for nozzle simulation on airplane force models.

5) At typical force-model nozzle plug diameters, plug recontouring has virtually no effect on boattail drag, although at much larger diameters some effects are observed. Although it was hoped that re-contouring of the force-model nozzle plug might bring boattail drag into closer agreement with the level of the engine conical plug-type nozzle, this method is found ineffective.

References

[1] Bergman, D., "Effects of Engine Exhaust Flow on Boattail Drag," *Journal of Aircraft*, Vol. 8, No. 6, June 1971, pp. 434–443.

[2] Shrewsbury, G. D., "Effect of Boattail Juncture Shape on Pressure Drag Coefficients of Isolated Afterbodies," TM X-1517, March 1968, NASA.